

Measurement of parity violation in electron–quark scattering

The Jefferson Lab PVDIS Collaboration*

Symmetry permeates nature and is fundamental to all laws of physics. One example is parity (mirror) symmetry, which implies that flipping left and right does not change the laws of physics. Laws for electromagnetism, gravity and the subatomic strong force respect parity symmetry, but the subatomic weak force does not^{1,2}. Historically, parity violation in electron scattering has been important in establishing (and now testing) the standard model of particle physics. One particular set of quantities accessible through measurements of parity-violating electron scattering are the effective weak couplings C_{2q} sensitive to the quarks' chirality preference when participating in the weak force, which have been measured directly^{3,4} only once in the past 40 years. Here we report a measurement of the parity-violating asymmetry in electron–quark scattering, which yields a determination of $2C_{2u} - C_{2d}$ (where u and d denote up and down quarks, respectively) with a precision increased by a factor of five relative to the earlier result. These results provide evidence with greater than 95 per cent confidence that the C_{2q} couplings are non-zero, as predicted by the electroweak theory. They lead to constraints on new parity-violating interactions beyond the standard model, particularly those due to quark chirality. Whereas contemporary particle physics research is focused on high-energy colliders such as the Large Hadron Collider, our results provide specific chirality information on electroweak theory that is difficult to obtain at high energies. Our measurement is relatively free of ambiguity in its interpretation, and opens the door to even more precise measurements in the future.

In parity-violating electron scattering (PVES) experiments, an asymmetry is measured that can be expressed as

$$A_{\text{PV}} = \frac{\sigma_{\text{R}} - \sigma_{\text{L}}}{\sigma_{\text{R}} + \sigma_{\text{L}}} \quad (1)$$

where $\sigma_{\text{R}}(\sigma_{\text{L}})$ are the cross-sections for scattering longitudinally polarized electrons that are in the right-handed R (left-handed L) helicity state, meaning their spins are parallel (antiparallel) to the electron's momentum. For deep inelastic scattering (DIS) from nuclear targets (DIS is defined as scattering in which the electron interacts with a single quark, almost independent of the surrounding quarks and gluons), this asymmetry can be written in a largely model-independent way as⁵

$$A_{\text{PV}} = \frac{G_{\text{F}} Q^2}{4\sqrt{2}\pi\alpha} [a_1(x, Q^2) Y_1(x, y, Q^2) + a_3(x, Q^2) Y_3(x, y, Q^2)] \quad (2)$$

where G_{F} is the Fermi constant, α is the fine-structure constant, $Q^2 \equiv -q^2$ with q the four-momentum transferred from the electron to the target, x is the Bjorken scaling variable and describes the fraction of momentum carried by the quark struck by the electron, $y = (E - E')/E$ is the fractional energy loss of the electron with $E(E')$ the incident (scattered) electron energy, $Y_{1,3}$ are kinematic factors, and the variables $a_{1,3}$ are related to the subatomic structure of the target. (See Supplementary Methods for a complete description.) The first experiment (SLAC E122) to detect parity violation in electron scattering^{3,4} provided results that strongly favoured the model of refs 6–8, establishing it as the keystone

of the now highly successful standard model of particle physics. PVES has subsequently been used as a sensitive probe to study diverse physics, ranging from physics beyond the standard model^{9,10} to the structure of both nuclei¹¹ and the nucleon (ref. 12 and references therein).

In so-called tree-level scattering, where the electron exchanges only a single photon or a single Z boson with the target, very simple expressions for $a_{1,3}$ in equation (2) emerge for electron DIS from deuterium:

$$a_1 = \frac{6}{5}(2C_{1u} - C_{1d}), \quad a_3 = \frac{6}{5}(2C_{2u} - C_{2d}) \quad (3)$$

The use of the deuterium target simplifies the interpretation because it has equal numbers of up and down valence quarks. Here, $C_{1u(1d)}$ and $C_{2u(2d)}$ are the effective weak couplings between the electrons and the up (down) quarks, often collectively written as C_{1q} and C_{2q} . The subscripts 1 and 2 refer to whether the coupling to the electron or quark is vector or axial-vector in nature: $C_{1u(d)}$ is the (AV) combination of the electron's axial-vector weak charge and the quark's vector weak charge, that is, it probes parity violation caused by the difference in the Z^0 coupling between left- and right-handed electron chiral states; $C_{2u(d)}$ is the (VA) combination of the electron's vector weak charge and the quark's axial-vector weak charge that is sensitive to parity violation due to the different quark chiral states. In testing the standard model it is important to determine all four $C_{1u,1d,2u,2d}$ as accurately as possible, because new interactions could manifest themselves in either set of couplings. Experimentally, one could extract both $2C_{1u} - C_{1d}$ and $2C_{2u} - C_{2d}$ by measuring asymmetries at different $Y_{1,3}$ values in the DIS regime. However, a precise determination of $2C_{2u} - C_{2d}$ is difficult because of its small value in the standard model (-0.095), as opposed to $2C_{1u} - C_{1d} = -0.719$.

The new measurement reported here was performed using the electron beam at the Thomas Jefferson National Accelerator Facility (referred to here as Jefferson Lab), in Virginia, USA. A 100- μA , nearly 90%-longitudinally-polarized electron beam was incident on a 20-cm-long liquid deuterium target held at a temperature of 22 K. Scattered particles were detected in a pair of magnetic spectrometers that determined the momentum and the direction of the detected particles to high precision¹³. To directly access $C_{2u,2d}$, the kinematics were chosen so that the bulk of the detected electrons emerged from the target after undergoing a DIS interaction. In contrast, all other PVES experiments after SLAC E122 were performed outside the DIS regime, and thus could not provide clean information on C_{2q} .

The size of the asymmetry expected for this measurement is at the level of 10^{-4} . The major challenge comes from the combination of the high electron event rate, and the high pion background typical of DIS measurements. This was overcome by the use of a custom electronic and data acquisition (DAQ) system with built-in pion rejection capability¹⁴. The DAQ system successfully counted electrons, event-by-event, at rates up to 600 kHz. The relative uncertainty in the measured asymmetries due to pion background was less than 5×10^{-4} , and that due to counting deadtime was less than 0.4%. The leading systematic uncertainty comes from the normalization by the electron beam polarization, which had a relative uncertainty of (1.2–1.8)%. Beam instability was

*Lists of participants and their affiliations appear at the end of the paper.

not a significant issue because of recent advances in the monitoring and feedback control of the beam, a direct outcome of some of the earlier PVES studies^{9–12}.

The high intensity of the Jefferson Lab beam allowed the completion of the experiment in just under two months. A total of about 170,000 million scattered electrons were counted at two DIS settings. The asymmetry measured at $E = 6.067$ GeV, $\langle x \rangle = 0.241$, $Y_1 = 1.0$, $Y_3 = 0.44$ and $\langle Q^2 \rangle = 1.085$ (GeV c^{-1})² was

$$A_{\text{exp}} = [-91.1 \pm 3.1(\text{stat.}) \pm 3.0(\text{syst.})] \times 10^{-6} \quad (4)$$

where $\langle x \rangle$ and $\langle Q^2 \rangle$ are averaged over the spectrometer acceptance, and stat. and syst. indicate statistical and systematic errors, respectively. This result is to be compared with the standard model (SM) expectation of $A_{\text{SM}} = -87.7 \times 10^{-6}$, with an uncertainty of 0.7×10^{-6} dominated by the uncertainty in the parton distribution functions (PDFs), parameterizations of how partons (quarks and gluons) that form the nucleon carry the nucleon's energy. To allow an extraction of $C_{1u,1d}$ and $C_{2u,2d}$ it is necessary to express the asymmetry in terms of these couplings. This relation was calculated using the MSTW2008 leading-order PDF parametrization¹⁵. For the kinematics above, it gives $A_{\text{SM}} = (1.156 \times 10^{-4}) [(2C_{1u} - C_{1d}) + 0.348(2C_{2u} - C_{2d})]$, where the relative uncertainties of the coefficients for the $(2C_{1u} - C_{1d})$ and the $(2C_{2u} - C_{2d})$ terms are 0.5% and 5%, respectively. The second DIS setting was at $E = 6.067$ GeV, $\langle x \rangle = 0.295$, $Y_1 = 1.0$, $Y_3 = 0.69$, $\langle Q^2 \rangle = 1.901$ (GeV c^{-1})², and the result was:

$$A_{\text{exp}} = [-160.8 \pm 6.4(\text{stat.}) \pm 3.1(\text{syst.})] \times 10^{-6} \quad (5)$$

The standard model expectation is $A_{\text{SM}} = (-158.9 \pm 1.0) \times 10^{-6}$. The coupling sensitivity is $A_{\text{SM}} = (2.022 \times 10^{-4}) [(2C_{1u} - C_{1d}) + 0.594(2C_{2u} - C_{2d})]$, with the same relative uncertainties as the first DIS setting. Details of the standard model calculation and the uncertainty due to PDF fits are given in Supplementary Methods.

Using the most recent world data for the coupling $C_{1u,1d}$ (ref. 16), obtained from PVES and caesium atomic parity violation experiments^{17–20}, a simultaneous fit of $2C_{1u} - C_{1d}$ and $2C_{2u} - C_{2d}$ to our results and to the asymmetries from SLAC E122 was performed, yielding:

$$\begin{aligned} (2C_{2u} - C_{2d})|_{Q^2=0} &= -0.145 \pm 0.066(\text{exp.}) \\ &\pm 0.011(\text{PDF}) \pm 0.012(\text{HT}) \\ &= -0.145 \pm 0.068(\text{total}) \end{aligned} \quad (6)$$

Here, exp. refers to the total experimental uncertainty, given by the statistical and the systematic uncertainties of the asymmetry results added in quadrature. The third uncertainty is due to the so-called higher-twist (HT) effects, caused by interactions among quarks inside the target. Further theoretical uncertainties, including QED vacuum polarization and the γZ box diagram, are negligible compared to the uncertainty due to the PDF fits. Electroweak and process-specific radiative corrections have been applied to calculate the values at zero- Q^2 , $C_{2u,2d}|_{Q^2=0}$ called $g_{\text{VA}}^{\text{eu,ed}}$ with e referring to electrons (and similarly $C_{1u,1d}|_{Q^2=0}$ called $g_{\text{AV}}^{\text{eu,ed}}$) in ref. 21, so that the values in equation (6) can be compared directly to results from other precision experiments using different kinds of processes. The values for $C_{2u,2d}|_{Q^2=0}$ differ from those at both Q^2 accessed in this experiment by 0.002–0.003 for both the up and the down quarks.

The asymmetry results in equations (4) and (5) can also be interpreted as a determination of the weak mixing angle θ_W , an important ingredient of the electroweak unification of the standard model. The result, evolved to the mass of the Z boson in the modified minimal subtraction ($\overline{\text{MS}}$) scheme, is $\sin^2 \theta_W(Q^2 = M_Z^2, \overline{\text{MS}}) = 0.2299 \pm 0.0043$, in agreement with the latest standard-model fit to world data, $\sin^2 \theta_W = 0.23126 \pm 0.00005$.

The result in equation (6) is compared with the standard-model prediction $2C_{2u} - C_{2d}|_{Q^2=0} = -0.0950 \pm 0.0004$ in Fig. 1. Our results have greatly improved the uncertainty on the effective electron–quark VA weak couplings $C_{2u,2d}$ and are in good agreement with the standard-model

prediction. This is also the first direct measurement of the coupling combination $2C_{2u} - C_{2d}$ that deviates from zero. We note that evidence for non-zero values of the $C_{2u,2d}$, possibly in a different combination from what we measured, may have been observed in experiments measuring the nucleon axial form factors²². However, extraction of $C_{2u,2d}$ from the nucleon axial form factor is model-dependent, whereas in DIS the electron probes quarks unambiguously. The directness of our approach is essential to reach a significantly higher accuracy in the future, such as through the PVDIS programme planned for the 12 GeV upgrade of Jefferson Lab.

A comparison of the present result with the standard-model predictions can be used to set mass limits Λ below which new interactions are unlikely to occur. For the cases of electron and quark compositeness and contact interactions, we used the convention of ref. 23 and the procedure in ref. 24. The limit for the constructive (destructive) interference contribution to the standard model is:

$$\Lambda^\pm = v \left[\frac{8\sqrt{5}\pi}{|(2C_{2u} - C_{2d})_{Q^2=0}|^\pm} \right]^{1/2} \quad (7)$$

where $|(2C_{2u} - C_{2d})_{Q^2=0}|^\pm$ is the difference between the standard-model value and the upper (lower) confidence bound of the data, $v = \sqrt{\sqrt{2}/(2G_F)} = 246.22$ GeV is the Higgs vacuum expectation value setting the electroweak scale, and the $\sqrt{5}$ is a normalization factor taking into account the coefficients of the $C_{2u,2d}$ in the denominator.

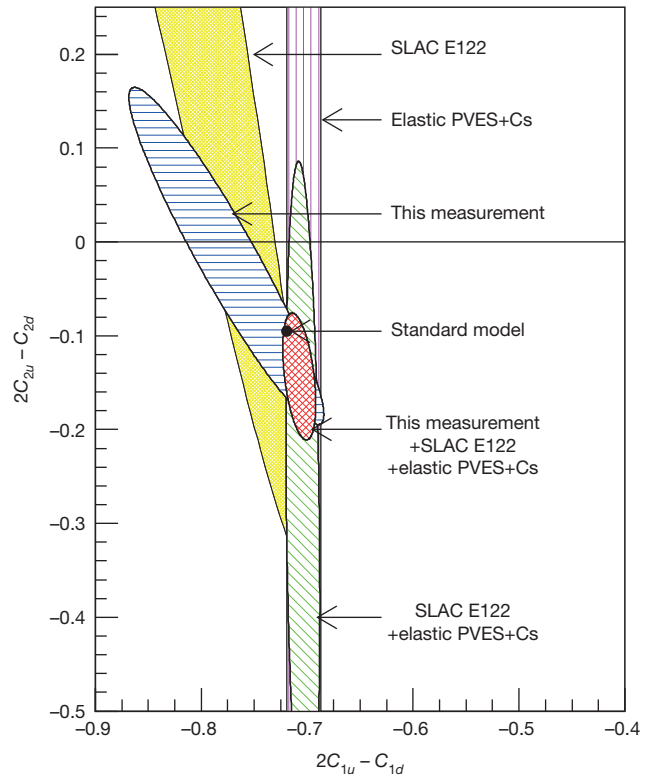


Figure 1 | Comparison of the present results with those of earlier experiments and predictions of the standard model. Values of $(2C_{1u} - C_{1d})|_{Q^2=0}$ and $(2C_{2u} - C_{2d})|_{Q^2=0}$ from this experiment (ellipse with blue horizontal hatching) are compared with those of SLAC E122 (yellow ellipse)^{3,4}. The latest data on C_{1q} (from PVES¹⁶ and atomic Cs^{17–20}) are shown as the band with magenta vertical hatching. The ellipse with diagonal green hatching shows the combined result of SLAC E122 and the latest C_{1q} , while the ellipse with red cross-hatching shows the combined result of SLAC E122, this experiment, and the latest C_{1q} . The standard model value (with negligible uncertainty) is shown as the black dot, where the size of the dot is for visibility.

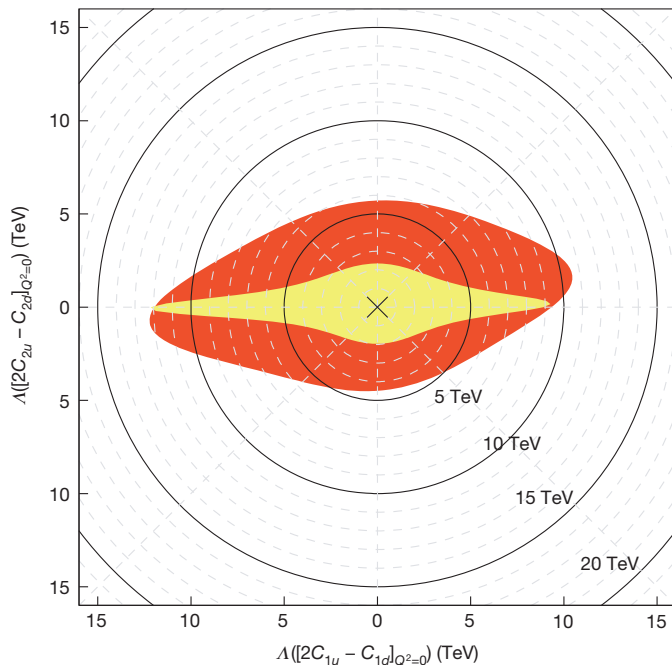


Figure 2 | Mass exclusion limits Λ on the electron and quark compositeness and contact interactions. These limits are obtained from the zero- Q^2 values of $2C_{1u} - C_{1d}$ and $2C_{2u} - C_{2d}$ at the 95% confidence level. The outside of the yellow shape shows the limit obtained from SLAC E122 asymmetry results^{3,4} combined with the best C_{1q} values¹⁶. The outside of the red shape shows the limit with our new results added. For visual guidance, mass limit scales in TeV are shown as solid and dashed circles.

For a 95% confidence level, we extracted

$$\Lambda^+ = 5.8 \text{ TeV} \quad \text{and} \quad \Lambda^- = 4.6 \text{ TeV} \quad (8)$$

for constructive and destructive interference from beyond-the-standard-model physics. Figure 2 illustrates these limits. The limits set by $C_{1u,1d}$ are determined mostly by previous PVES and caesium atomic-parity-violation results, but this experiment clearly improves the limits set by $C_{2u,2d}$.

The strength of our results reported here is that they isolate a well-defined combination of the electron–quark contact interactions. We note that mass limits on the electron–quark contact interactions have been published by the ZEUS²⁵ and H1²⁶ collaborations at the Hadron–Electron Ring Accelerator, HERA. They find $\Lambda^+ = 3.3 \text{ TeV}$ and $\Lambda^- = 3.2 \text{ TeV}$ (ref. 25), and $\Lambda^+ = 3.8 \text{ TeV}$ and $\Lambda^- = 3.6 \text{ TeV}$ (ref. 26), respectively, on the electron–quark VA term. Similar limits of $\Lambda^+ = 9.5 \text{ TeV}$ and $\Lambda^- = 12.1 \text{ TeV}$ have been published by the ATLAS collaboration²⁷ at the LHC in the left–left isoscalar model. To account for the different chirality structure of the models used, the HERA limits on the electron–quark VA model need to be scaled by $2^{-1/4} = 0.84$, while the LHC limits using the left–left isoscalar model need to be scaled by $2^{1/4} = 1.19$, in order to be compared to the mass limits extracted from $C_{2u,2d}$. The HERA and the LHC measurements are sensitive to several different vector and axial–vector weak charge combinations, thus their limits were obtained with the assumption that, apart from the particular chirality combination used in the model, all other contact interactions are zero. This assumption is unnecessary for the extraction of mass limits from our results. The chiral structure of the effective electron–quark weak couplings C_{2q} isolates interactions beyond the standard model in which it is the chirality of the quarks that is responsible for the observed parity violation.

METHODS SUMMARY

The parity-violating asymmetry A_{exp} between right- and left-handed electrons was computed from the detected counts C , normalized by the beam intensity I , and

integrated over periods of stable beam helicity. Two kinds of corrections were then made to the asymmetries: overall normalization factors and possible systematic shifts due to false asymmetries arising from backgrounds or helicity correlations in the beam parameters. The normalization factors include the beam polarization, measurements of scattered-electron kinematics, electromagnetic radiative corrections, and effects from two-photon exchange between the electron and target. The false-asymmetry corrections were all very small compared to the statistical error and included an evaluation of helicity correlations in beam current, position and energy, and backgrounds such as pions, scattering from the target aluminium windows, or rescattering inside the spectrometers. A summary of all corrections and the asymmetry results is presented in Supplementary Table 1.

To calculate the standard-model expectation of the measured asymmetry and its sensitivity to $2C_{1u} - C_{1d}$ and $2C_{2u} - C_{2d}$, we used PDFs to calculate the structure functions in $a_{1,3}$. Three PDF fits were used. Results of the calculation are shown in Supplementary Table 2. The relative variation among all three fits is less than 0.6% for the a_1 term, and less than 5% for the a_3 term of the asymmetry. Effects from interactions among quarks inside the target, called ‘higher-twist effects’, were evaluated using the most recent theoretical bounds combined with data on neutrino structure functions. It was found that the uncertainty in the extraction of $2C_{2u} - C_{2d}$ due to the higher-twist effects is at the same level as that due to the PDFs, and is quite small compared to the experimental uncertainties.

Received 28 October; accepted 17 December 2013.

- Lee, T. D. & Yang, C.-N. Question of parity conservation in weak interactions. *Phys. Rev.* **104**, 254–258 (1956).
- Wu, C. S., Ambler, E., Hayward, R. W., Hoppes, D. D. & Hudson, R. P. Experimental test of parity conservation in beta decay. *Phys. Rev.* **105**, 1413–1415 (1957).
- Prescott, C. Y. *et al.* Parity nonconservation in inelastic electron scattering. *Phys. Lett. B* **77**, 347–352 (1978).
- Prescott, C. Y. *et al.* Further measurements of parity nonconservation in inelastic electron scattering. *Phys. Lett. B* **84**, 524–528 (1979).
- Cahn, R. N. & Gilman, F. J. Polarized-electron-nucleon scattering in gauge theories of weak and electromagnetic interactions. *Phys. Rev. D* **17**, 1313–1322 (1978).
- Glashow, S. L. Partial symmetries of weak interactions. *Nucl. Phys.* **22**, 579–588 (1961).
- Weinberg, S. A model of leptons. *Phys. Rev. Lett.* **19**, 1264–1266 (1967).
- Salam, A. Weak and electromagnetic interactions. In *Elementary Particle Theory: Relativistic Groups and Analyticity* (ed. Svartholm, N.) 367–377 (Almqvist and Wiksell, 1968).
- Anthony, P. L. *et al.* Precision measurement of the weak mixing angle in Moller scattering. *Phys. Rev. Lett.* **95**, 081601 (2005).
- Czarnecki, A. & Marciano, W. J. Electrons are not ambidextrous. *Nature* **435**, 437–438 (2005).
- Abrahamyan, S. *et al.* Measurement of the neutron radius of ²⁰⁸Pb through parity-violation in electron scattering. *Phys. Rev. Lett.* **108**, 112502 (2012).
- Armstrong, D. S. & McKeown, R. D. Parity-violating electron scattering and the electric and magnetic strange form factors of the nucleon. *Annu. Rev. Nucl. Part. Sci.* **62**, 337–359 (2012).
- Alcorn, J. *et al.* Basic instrumentation for Hall A at Jefferson Lab. *Nucl. Instrum. Methods A* **522**, 294–346 (2004).
- Subedi, R. *et al.* A scaler-based data acquisition system for measuring parity violation asymmetry in deep inelastic scattering. *Nucl. Instrum. Methods A* **724**, 90–103 (2013).
- Martin, A. D., Stirling, W. J., Thorne, R. S. & Watt, G. Parton distributions for the LHC. *Eur. Phys. J. C* **63**, 189–285 (2009).
- Androic, D. *et al.* First determination of the weak charge of the proton. *Phys. Rev. Lett.* **111**, 141803 (2013).
- Wood, C. S. *et al.* Measurement of parity nonconservation and an anapole moment in cesium. *Science* **275**, 1759–1763 (1997).
- Bennett, S. C. & Wieman, C. E. Measurement of the ⁶S → ⁷S transition polarizability in atomic cesium and an improved test of the Standard Model. *Phys. Rev. Lett.* **82**, 2484–2487 (1999); erratum **83**, 889 (1999).
- Ginges, J. S. M. & Flambaum, V. V. Violations of fundamental symmetries in atoms and tests of unification theories of elementary particles. *Phys. Rep.* **397**, 63–154 (2004).
- Dzuba, V. A., Berengut, J. C., Flambaum, V. V. & Roberts, B. Revisiting parity nonconservation in cesium. *Phys. Rev. Lett.* **109**, 203003 (2012).
- Erler, J. & Su, S. The weak neutral current. *Prog. Part. Nucl. Phys.* **71**, 119–149 (2013).
- Beise, E. J., Pitt, M. L. & Spayde, D. T. The SAMPLE experiment and weak nucleon structure. *Prog. Part. Nucl. Phys.* **54**, 289–350 (2005).
- Eichten, E., Lane, K. D. & Peskin, M. E. New tests for quark and lepton substructure. *Phys. Rev. Lett.* **50**, 811–814 (1983).
- Schael, S. *et al.* Electroweak measurements in electron-positron collisions at W -boson-pair energies at LEP. *Phys. Rep.* **532**, 119–244 (2013).
- Chekanov, S. *et al.* Search for contact interactions, large extra dimensions and finite quark radius in ep collisions at HERA. *Phys. Lett. B* **591**, 23–41 (2004).
- Aaron, F. D. *et al.* Search for contact interactions in e^+p collisions at HERA. *Phys. Lett. B* **705**, 52–58 (2011).

27. Aad, G. *et al.* Search for contact interactions and large extra dimensions in dilepton events from pp collisions at $\sqrt{s}=7$ TeV with the ATLAS detector. *Phys. Rev. D* **87**, 015010 (2013).

Supplementary Information is available in the online version of the paper.

Acknowledgements We thank the personnel of Jefferson Lab for their efforts which resulted in the successful completion of the experiment, and A. Accardi, P. Blunden, W. Melnitchouk and their collaborators for carrying out the calculations necessary for the completion of the data analysis. X.Z. thanks the Medium Energy Physics Group at the Argonne National Laboratory for support during the initial work on this experiment. J.E. was supported by PAPIIT (DGAPAUNAM) project IN106913 and CONACyT (México) project 151234, and acknowledges the hospitality and support by the Mainz Institute for Theoretical Physics (MITP) where part of his work was completed. This work was supported in part by the Jeffress Memorial Trust (award no. J-836), the US NSF (award no. 0653347), and the US DOE (award nos DE-SC0003885 and DE-AC02-06CH11357). This work was authored by Jefferson Science Associates, LLC under US DOE contract no. DE-AC05-06OR23177. The US Government retains a non-exclusive, paid-up, irrevocable, world-wide license to publish or reproduce this manuscript for US Government purposes.

Author Contributions Authors contributed to one or more of the following areas: proposing, leading, and running the experiment; design, construction, optimization, and testing of the data acquisition system; data analysis; simulation; extraction of the physics results from measured asymmetries; and the writing of this Letter.

Author Information J.E. is currently on sabbatical leave at the PRISMA Cluster of Excellence and MITP, Johannes Gutenberg University. Reprints and permissions information is available at www.nature.com/reprints. The authors declare no competing financial interests. Readers are welcome to comment on the online version of the paper. Correspondence and requests for materials should be addressed to X.Z. (xz5y@virginia.edu).

The Jefferson Lab PVDIS Collaboration

D. Wang¹, K. Pan², R. Subedi^{1†}, X. Deng¹, Z. Ahmed³, K. Allada⁴, K. A. Aniol⁵, D. S. Armstrong⁶, J. Arrington⁷, V. Bellini⁸, R. Beminiwattha⁹, J. Benesch¹⁰, F. Benmokhtar¹¹, W. Bertozzi², A. Camsonne¹⁰, M. Canan¹², G. D. Cates¹, J.-P. Chen¹⁰, E. Chudakov¹⁰, E. Cisbani¹³, M. M. Dalton¹, C. W. de Jager^{1,10}, R. De Leo¹⁴, W. Deconinck^{2†}, A. Deur¹⁰, C. Dutta⁴, L. El Fassi¹⁵, J. Erler¹⁶, D. Flay¹⁷, G. B. Franklin¹¹, M. Friend¹¹, S. Frullani¹³, F. Garibaldi¹³, S. Gilad², A. Giusa⁸, A. Glamazdin¹⁸, S. Golge¹², K. Grimm¹⁹, K. Hafidi⁷, J.-O. Hansen¹⁰, D. W. Higinbotham¹⁰, R. Holmes³, T. Holmstrom²⁰, R. J. Holt⁷, J. Huang²,

C. E. Hyde^{12,21}, C. M. Jen³, D. Jones¹, Hoyoung Kang²², P. M. King⁹, S. Kowalski², K. S. Kumar²³, J. H. Lee^{6,9}, J. J. LeRose¹⁰, N. Liyanage¹, E. Long²⁴, D. McNulty^{23†}, D. J. Margaziotis⁵, F. Meddi²⁵, D. G. Meekins¹⁰, L. Mercado²³, Z.-E. Meziani¹⁷, R. Michaels¹⁰, M. Mihovilovic²⁶, N. Muangma², K. E. Myers^{27†}, S. Nanda¹⁰, A. Narayan²⁸, V. Nelyubin¹, Nuruzzaman²⁸, Y. Oh²², D. Parno¹¹, K. D. Paschke¹, S. K. Phillips²⁹, X. Qian³⁰, Y. Qiang³⁰, B. Quinn¹¹, A. Rakhman³, P. E. Reimer⁷, K. Rider²⁰, S. Riordan¹, J. Roche⁹, J. Rubin⁷, G. Russo³, K. Saenboonruang^{1†}, A. Saha^{10†}, B. Sawatzky¹⁰, A. Shahinyan³¹, R. Silwal¹, S. Sirca²⁶, P. A. Souder³, R. Suleiman¹⁰, V. Sulkosky², C. M. Suter⁸, W. A. Tobias¹, G. M. Urciuoli²⁵, B. Waidyawansa⁹, B. Wojtsekhowski¹⁰, L. Ye³², B. Zhao⁵ & X. Zheng¹

¹University of Virginia, Charlottesville, Virginia 22904, USA. ²Massachusetts Institute of Technology, Cambridge, Massachusetts 02139, USA. ³Syracuse University, Syracuse, New York 13244, USA. ⁴University of Kentucky, Lexington, Kentucky 40506, USA. ⁵California State University, Los Angeles, Los Angeles, California 90032, USA. ⁶College of William and Mary, Williamsburg, Virginia 23187, USA. ⁷Physics Division, Argonne National Laboratory, Argonne, Illinois 60439, USA. ⁸Istituto Nazionale di Fisica Nucleare, Dipt. di Fisica dell'Univ. di Catania, I-95123 Catania, Italy. ⁹Ohio University, Athens, Ohio 45701, USA. ¹⁰Thomas Jefferson National Accelerator Facility, Newport News, Virginia 23606, USA. ¹¹Carnegie Mellon University, Pittsburgh, Pennsylvania 15213, USA. ¹²Old Dominion University, Norfolk, Virginia 23529, USA. ¹³INFN, Sezione di Roma, gruppo Sanità and Istituto Superiore di Sanità, I-00161 Rome, Italy. ¹⁴Università di Bari, I-70126 Bari, Italy. ¹⁵Rutgers, The State University of New Jersey, Newark, New Jersey 07102, USA. ¹⁶Instituto de Física, Universidad Nacional Autónoma de México, 04510 México D.F., Mexico. ¹⁷Temple University, Philadelphia, Pennsylvania 19122, USA. ¹⁸Kharkov Institute of Physics and Technology, Kharkov 61108, Ukraine. ¹⁹Louisiana Technical University, Ruston, Louisiana 71272, USA. ²⁰Longwood University, Farmville, Virginia 23909, USA. ²¹Clermont Université, Université Blaise Pascal, CNRS/IN2P3, Laboratoire de Physique Corpusculaire, FR-63000 Clermont-Ferrand, France. ²²Seoul National University, Seoul 151-742, South Korea. ²³University of Massachusetts Amherst, Amherst, Massachusetts 01003, USA. ²⁴Kent State University, Kent, Ohio 44242, USA. ²⁵INFN, Sezione di Roma and Sapienza — Università di Roma, I-00161 Rome, Italy. ²⁶Institut Jožef Stefan, SI-1001 Ljubljana, Slovenia. ²⁷George Washington University, Washington DC 20052, USA. ²⁸Mississippi State University, Starkville, Mississippi 39762, USA. ²⁹University of New Hampshire, Durham, New Hampshire 03824, USA. ³⁰Duke University, Durham, North Carolina 27708, USA. ³¹Yerevan Physics Institute, Yerevan 0036, Armenia. ³²China Institute of Atomic Energy, Beijing 102413, China. †Present addresses: Richland College, Dallas County Community College District, Dallas, Texas 75243, USA (R.S.); College of William and Mary, Williamsburg, Virginia 23187, USA (W.D.); Idaho State University, Pocatello, Idaho 83201, USA (D.M.); Rutgers, The State University of New Jersey, Newark, New Jersey 07102, USA (K.E.M.); Kasetsart University, Bangkok 10900, Thailand (K.S.).

‡Deceased.